High Surface Area and Photo-catalysis of $Cu_{0.3}Cd_{0.7}CrFeO_4$ Nanocrystals in Degradation of Methylene Blue (MB)

Amina Ibrahim Ghoneim*

Physics Department, Faculty of Science, Tanta University, Tanta 31527, Egypt

Abstract

$Cu_{0.3}Cd_{0.7}CrFeO_4$ nanocrystals were obtained via co-precipitation strategy, and well-precisely scrutinized. XRD scrutiny affirmed the egress of the Nano-spinel phase for these nanocrystals existing in the Nano-regime. The teeny crystallite size R average value was 10.55 nm. All deduced parameters were affected by coexistence of Cu^{2+}, Cd^{2+}, Fe^{2+}, Cr^{3+} and Fe^{3+} cations inside these nanocrystals. HRTEM images showed no accumulations for these Nano-spinels, where the average particle size value was 11.11 nm and was slightly bigger than the crystallite size R. Evaluation of photocatalytic activity for **$Cu_{0.3}Cd_{0.7}CrFeO_4$** Nano-spinel was acquired throughout the disintegration of Methylene Blue (**MB**) dye (1×10^{-3} M and 2×10^{-3} M) in aqueous medium under visible light (VL) irradiation using 100 Watt Tungsten lamp fixed at ~ 10 cm distance. As a result, usage of these new ultrafine **$Cu_{0.3}Cd_{0.7}CrFeO_4$** nanocrystals gives a new marvellous route for the advancement of cost-effective technologies for quite good waste H_2O recycling models, for raising H_2O quality and for the promotion of fruitful efforts in improving treatment systems.

Keywords:

$Cu_{0.3}Cd_{0.7}CrFeO_4$ nanocrystals; HRTEM; Methylene Blue (**MB**); Photo-degradation; water treatment

Paper information:

Receive Date: 25 October 2021; Revise Date: 22 December 2021; Accept Date: 29 December 2021; Publish Date: 30 December 2021.

Corresponding Authors (*): mona_ghoneim@yahoo.com, amina.ali@science.tanta.edu.eg

1. Introduction

Photo-catalysis progression for impure H2O treating is a serious target for environmentally ongoing inspection endeavors. Nano-spinels are soft-magnetic semiconducting nanocrystals possessing supreme persistence, and distinctly economical; thence these Nano-spinels are facilely fabricated and possess prevalent utilizations in marvellous prospects in NTC thermistors, electronical industries, magnetic refrigeration, ferrofluids and satellite communications [1-3]. Photo-catalytic efficacy for dye disintegration under visible light photons has exceedingly scrutinized within recent times. Organic dyes are vastly utilized in plentiful industries producing serious impact in nature causing adverse leverage on environmental prospects. Obviously, disintegration of such dyes is so serious, where disintegration via photo-catalysing is one of the most efficacious strategies for H_2O up-cleaning [4]. Semiconducting photocatalytic strategy had targeted a marvellous route for environmentally polluted treating imputing to their entire disintegrations from organic contaminations into CO_2 and H_2O at ambient status [5]. Nano-spinels are utilized as one of prospective and gorgeous semiconducting nanocrystals; thence they have animated gorgeous scrutiny vistas imputing to their eminent features. Persistent endeavors have been protracted to persuade photocatalytic achievement of Nano-spinels [6]. Scrutiny endeavours in Nano-science have utility toward diverse prospects such: fabrication, exploration of newfangled nanostructures [7,8].

Distinctly, usage of Nano-spinel is so efficacious in disintegration of organic dyes, where these nanocrystals raise the efficacy of this procedure. This aspect has been early emphasized by [8], utilizing $ZnFe_2O_4$ in this aspect confirming their impress in dye disintegration. Thus, current scrutiny targeted the fabrication of new nanocrystals ($\mathbf{Cu_{0.3}Cd_{0.7}CrFeO_4}$ Nano-spinels) and distinguishing their merits. The second main target is getting water cleaned via simple strategy as inspecting their ability in **MB** disintegration. Evaluation of photocatalytic activity for $\mathbf{Cu_{0.3}Cd_{0.7}CrFeO_4}$ Nano-ferrites was obtained

through the disintegration of **MB** in aqueous medium under VL irradiation using 100 Watt Tungsten lamp fixed at ~ 10 cm distance.

2. Experimental Techniques

2.1. Preparation of $Cu_{0.3}Cd_{0.7}CrFeO_4$ nanoparticles

As-prepared **$Cu_{0.3}Cd_{0.7}CrFeO_4$** Nano-spinels have been synthesized utilizing co-precipitation route according to the equation [9]:

$$0.3\ CuCl_2.2H_2O + 0.7\ CdCl_2\ H_2O + CrCl_3.6H_2O + FeCl_3 + 8\ NaOH \rightarrow Cu_{0.3}Cd_{0.7}CrFeO_4 + 11.3\ H_2O + 8NaCl$$

Co-precipitation methodology has been early reported [10]. Metal Chlorides are mixed together; then NaOH was added dropwise until PH=12; thence heated up to 80 ^oC/2h, thereafter precipitated, washed, dried, thence ground.

2.2. Characterizations:

Nano-ferrite powder was inspected via GNR APD 2000 Pro X-ray diffractometer step scan type and $CuK\alpha_1$ radiation at wavelength $\lambda = 1.540598$ Å [11]. FT-IR spectra was explored via Bruker-Tensor-27-FT-IR - type in the range from 200 to 2000 cm^{-1} [12,13]. Moreover, morphology was scrutinized via JEOL JEM – 2100 Electron Microscope. UV–vis spectra were registered using SPECTRO UV–VIS DUAL BEAM 8 AUTO CELL UVS-2700 scan-type spectrophotometer in the wavelengths 190 – 1200 nm at ambient temperature.

2.3. Photocatalytic activity of $Cu_{0.3}Cd_{0.7}CrFeO_4$ nanocrystals:

Photocatalytic features of **$Cu_{0.3}Cd_{0.7}CrFeO_4$** nanocrystals were scrutinized via photo-disintegration of the simulated dye wastewater of **MB** solution under VL irradiation utilizing 100 Watt Tungsten lamp fixed at ~ 10 cm distance, as illuminated in Fig. 1. Aqueous suspension of **MB-dye** (**1×10^{-3} M and 2×10^{-3} M**) and **$Cu_{0.3}Cd_{0.7}CrFeO_4$** nanocrystals as photo-catalysts (0.1 g) were placed in a glass beaker. Prior to irradiation, each suspension was stirred in dark for 2 hrs to establish adsorption-desorption equilibrium (between photo-catalysts and dye), followed by VL irradiation utilizing 100 Watt Tungsten lamp fixed at ~ 10 cm distance. At time spans (20 min), 3 mL of suspension was taken from beaker, and then filtered to remove solid powders. Thence, solutions analysed by UV–VIS scan-type photometer in the wavelengths 190 – 1200 nm at ambient temperature to obtain relative

concentration variations of solution. Curve about concentration variations ($\mathbf{C/C_o}$) as a function of time was plotted, where **C** presented concentration of **MB** at each time interval and $\mathbf{C_o}$ was initial concentration of **MB** after reaching adsorption-desorption equilibrium [14].

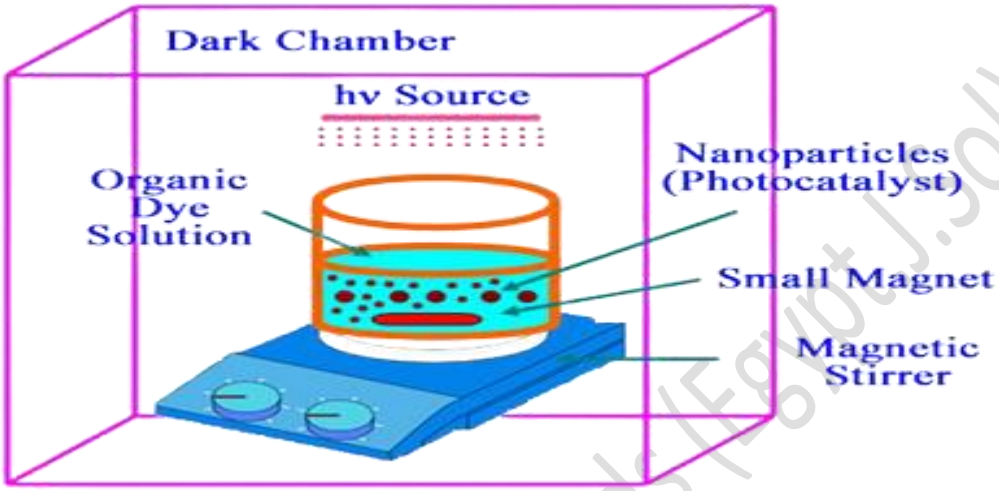

Fig. 1 Schematic illustration of the experimental apparatus setup used for Photo-Degradation mechanism of Methylene Blue (**MB**) over surface of ultrafine $\mathbf{Cu_{0.3}Cd_{0.7}CrFeO_4}$ Nanocrystals.

3. Results and discussion

3.1. X-ray diffracting plots (XRD)

$\mathbf{Cu_{0.3}Cd_{0.7}CrFeO_4}$ nanocrystals affirmed egress of Nano-spinel monocular-phase which was illustrated by XRD diagrams in Fig. 2. Protruded peaks belong to Nano-spinel which was affirmed by matching with JCPDS card no. 00-001-1111. Plainly, for teeny Nano-size merit of these Nano-samples; so that emerges relatively wider XRD summits in Fig. 2, as affirmed regarding the teeny crystallite sizes as pointed in Table 1. Lattice cons a is ranging ≈ 8.506 Å; agreeing with early scrutinized work [15]. Elucidated crystallite size R ranges ≈ 10.55 nm, in Nano-scale ambit [16].

Obviously, S discloses reliance on both R and X-ray density D_x, and ε relies on R. They possess big specified surface area S imputing to their teeny R [17]. S and ε values are illuminated in Table 1, matching well with early scrutiny [18]. Cell volume V and D_x are presented in Table 1.

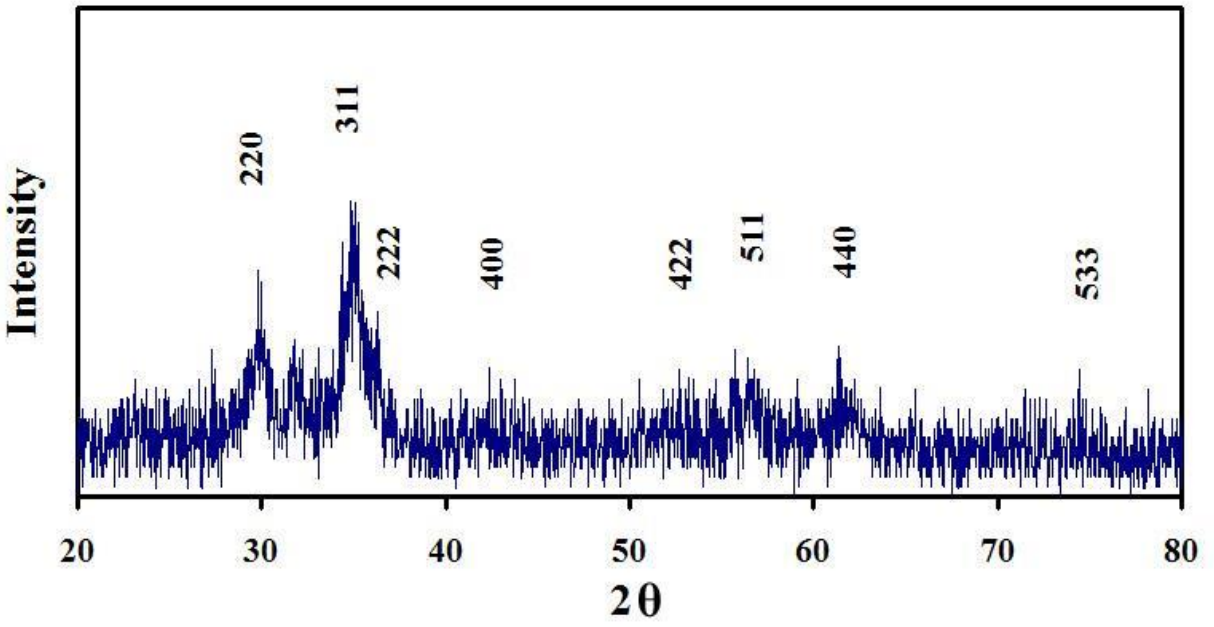

Fig. 2 XRD plots of As-Prepared Nano-spinel $\mathbf{Cu_{0.3}Cd_{0.7}CrFeO_4}$.

3.2. Structural Phase Analysis

3-Dimensional cell volume was contrived utilizing the formulation [19]; $V_{cell} = a^3$.

3-Dimensional cell volume V disclosed a precise value reaching ≈ 615.488 (Å)^3, (Table 1).

X-ray density was contrived via the formulation [20]: $D_X = \frac{ZM}{N_A V}$

, Z is molecules no. per unit cell (Z = 8); M is molecular weight and NA is Avogadro's no.

Dislocation density δ was contrived via expression [21]: $\delta = \frac{1}{R^2}$

Distortion parameter g was contrived via formulation [18,21]: $g = \frac{\beta_{1/2}}{\tan\theta}$

Table 1 discloses dependence of g and δ on R and θ, whilst g and δ depend on oxygen ion concentration [21].

Specified surface area S of Nano-spinels contrived via formulation [17,18];

$$S = \frac{6000}{R_{XRD} D_x}$$

Strain ε of Nano-spinels was contrived utilizing the formula [17,18];

$$\beta_{1/2}\cos\theta = \frac{0.94\lambda}{R_{XRD}} + 4\varepsilon\sin\theta$$

Strain ε interior these Nano-spinels affected by cations type and their crystalline configuration, (Table 1), as well as the protruded crystalline anisotropy [22]. Specified surface area S is ≈ 97.74 m^2/g, assigning to teeny R, (Table 1).

Table 1 Lattice parameter a, crystallite size R, strain ε, unit cell volume V, X-ray density D_x, specified surface area S, distortion parameter g and dislocation density δ, error = ± 0.02.

Nano-spinel	a (Å)	R (nm)	ε	V $(Å)^3$	D_x $(gm.cm^{-3})$	S (m^2/g)	g	δ $(nm^{-2}) \times 10^{-2}$
$Cu_{0.3}Cd_{0.7}CrFeO_4$	8.506	10.55	-0.098	615.488	5.818	97.74	0.0436	0.898

3.3. FT-IR Spectral plots

Infrared plot for $Cu_{0.3}Cd_{0.7}CrFeO_4$ nanocrystals was registered from 200 to 2000 cm^{-1} in Fig. 3. Protruded vibrational summits illuminated in Table 2. 6-summits of ν_1, ν_2, ν_4, ν_A, ν_B and ν_T egressed in FT-IR plots. ν_1 at 615.3 cm^{-1} and ν_2 at 501.5 cm^{-1}, (Table 2), referred to substantial sprawl oscillations of A-occupational allocations ligations; whereas enormous recapture strengths for bond-bending oscillations subsist on B-occupational allocations [23]. Predominately, affirmation of emersion of Nano-spinel configuration is affirmed by entity of both ν_1 and ν_2. Likewise, vibrational summit at 223.7 cm^{-1} for ν_4 referring to lattice oscillations and it relies on the ligaments, Fe^{2+} - O^{2-}, Cd^{2+} - O^{2-} and/or Cu^{2+} - O^{2-} [10,24]. Ternary summit ν_T at ~ 1638 cm^{-1} assigning to conserved H_2O in Nano-Crystals [25]. Summits around 910.4 and 1053 cm^{-1}, are pointing to supremes ν_A and ν_B. ν_A refer to coexistence of Fe^{2+}, Cd^{2+} amongst A- sites. ν_B refer to coexistence of Fe^{4+}-O^{2-} and Cr^{3+}-O^{2-}. Protrude of Fe^{4+} impute to electron jumping in-between Fe^{3+} and Cr^{3+} [10].

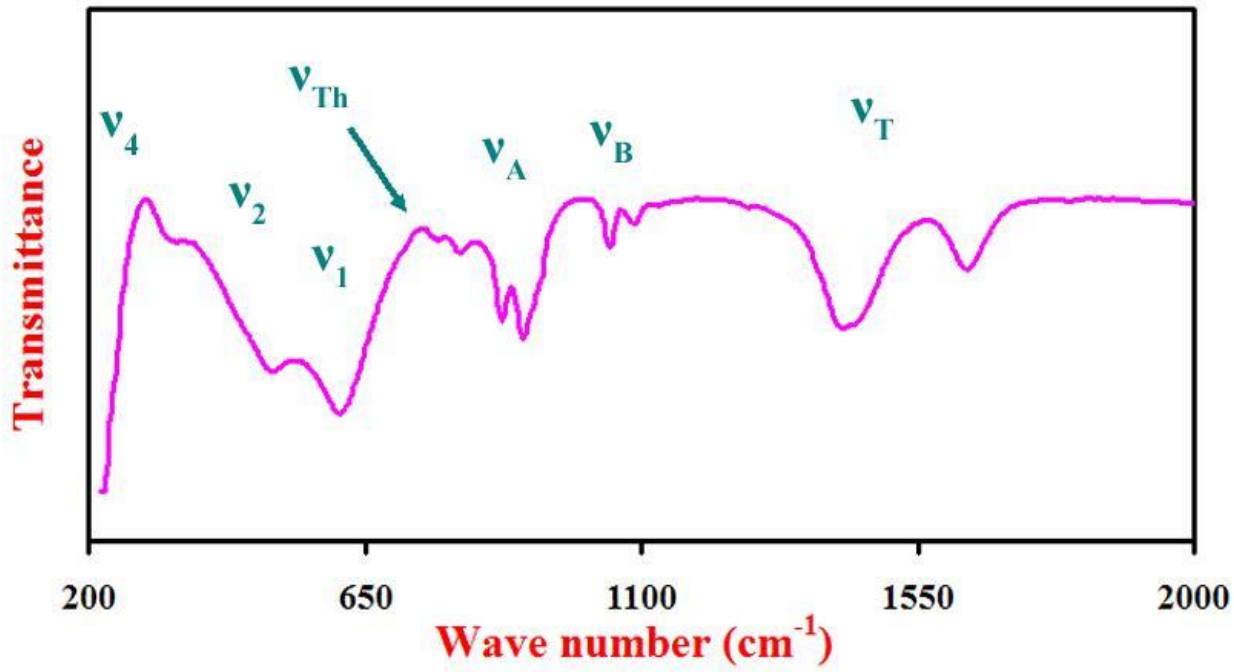

Fig. 3 FT-IR spectral plots of As-Prepared Nano-spinel **$Cu_{0.3}Cd_{0.7}CrFeO_4$**.

Debye temperature was deduced via the formulation [26]:

$$\theta_D = \frac{\hbar C \nu_{av}}{k} = 1.438 \nu_{av} \quad \text{and} \quad \nu_{AV} = \frac{\nu_1 + \nu_2}{2}$$

; ν_{av} is mean value of wave no's of oscillational supremes, ħ = h/2π, h is the Plank's cons, k is Boltzmann's cons, C = 3×10^{10} cm/s; C is light speed and $\hbar C/k$ = 1.438 for Nano-spinels [26]: θ_D nearly ≈ 802.95 K [27].

Concerning specified thermic theorem; the egress of conduction electrons portion (n-type transporters) procuring somewhat of thermic potency declining its saucepan, and this bolsters the connotation that conduction impute to electrons, and vice versa. Sill threshold frequency ν_{Th} is subsisting at 744.447 cm^{-1} assigning to transition electrons, whilst ν_{Th} can be picked up via supreme spot of FT-IR plots [26,27]; thence, conduction electron no's possess impact on ν_{Th} and θ_D. Force cons F_1 and F_2 equals 2.772 $\times10^5$ and 1.841 $\times10^5$ dyne/cm, assuring reliance of F_1 and F_2 on A- and B-sites oscillational frequencies, (Table 2).

Substantially, Threshold energy deduced via formulation [13]:

$$E_{Th} = hC\nu_{Th}$$

Deduced evaluation of ν_{Th} and E_{Th} are illuminated in Table 2.

Threshold supreme ν_{Th} emanated around 744.447 cm^{-1} conveying towards bigger frequencies assigning to high concentration of Fe^{2+} and Fe^{3+} and also assigning to hopping status as illuminated in the following expression:

$$Fe^{2+} + Fe^{4+} \leftrightarrow Fe^{3+}$$

The threshold energy E_{Th} possesses high evaluation as that of ν_{Th}, (Table 2).

Table 2 FT-IR vibrational summits positions ν_n; n = 1, 2,…and B, Threshold frequency ν_{Th}, Threshold energy E_{Th} (eV), Debye temperature Θ_D, Force con F_1 and F_2, error = ± 0.02.

Nano-spinel	ν_1 (cm^{-1})	ν_2 (cm^{-1})	ν_4 (cm^{-1})	ν_A (cm^{-1})	ν_B (cm^{-1})	ν_T (cm^{-1})	ν_{Th} (cm^{-1})	E_{Th} (eV)	Θ_D (K)	F_1 *10^5 (dyne/cm)	F_2 *10^5 (dyne/cm)
$Cu_{0.3}Cd_{0.7}CrFeO_4$	615.3	501.5	223.7	910.4	1053	1638	744.447	0.0925	802.95	2.772	1.841

3.4. HRTEM images

HRTEM pics of **$Cu_{0.3}Cd_{0.7}CrFeO_4$** Nano-spinels are illuminated in Fig. 4. These nanoparticles are not aggregated. Mean nanoparticle size Z reaches ≈ 11.11 nm. Z evaluation is closer to that of R [15,28].

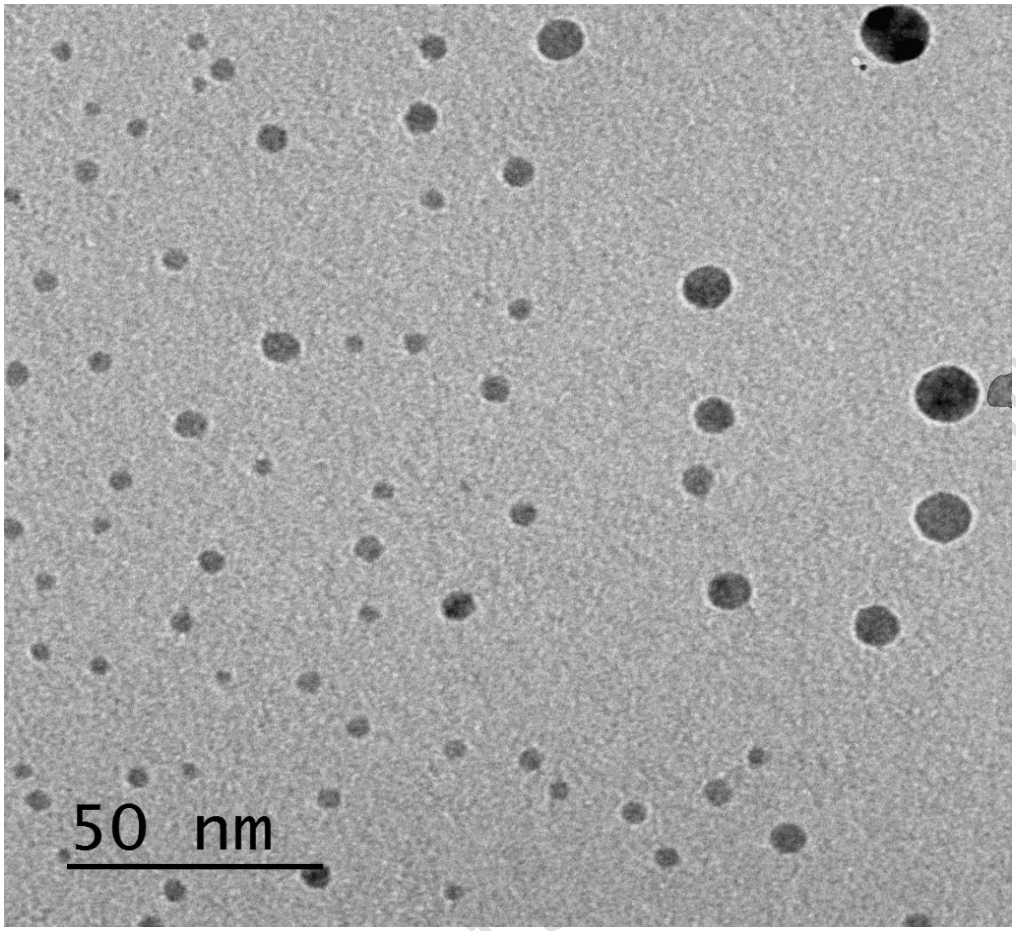

Fig. 4 HRTEM pics of As-prepared Nano-spinel $\mathbf{Cu_{0.3}Cd_{0.7}CrFeO_4}$.

3.5. Photocatalytic features:

Photo-catalytic activities of teeny $\mathbf{Cu_{0.3}Cd_{0.7}CrFeO_4}$ Nano-spinels for the sequent decolourization of Methylene Blue (**MB**) dye (**1×10^{-3} M and 2×10^{-3} M**) in aqueous solution under VL irradiation via 100 Watt Tungsten lamp fixed at ~ 10 cm distance, examined under surging of sequent spans of time up to 180 minutes, (time duration is 20 min) were affirmed in Fig. 5 and Fig. 6. All of the catalytic disintegration reactions followed pseudo-first-order kinetics, evidenced by plotting of (**C/Co**) against time (min), as well as plotting of **ln (C/Co)** against reaction time (min), (Fig. 5 and Fig. 6). It is explicit that, **MB** concentrations continuously decline with surge of stirring time emphasizing the photocatalytic activity of these Nano-spinels [29]. Disintegration Efficiency was elicited utilizing the following expression [30]:

$$Degradation - Efficiency = \left(1 - \frac{C}{C_o}\right) \times 100$$

Photo-catalytic efficiency of teeny **$Cu_{0.3}Cd_{0.7}CrFeO_4$** Nano-spinels for **MB** disintegration was explicitly explored on Fig. 5 and Fig. 6, proofing surging of their capability and activity in photo-degradation of **MB** dye, and referring to how high quality will be the treated H_2O by this procedure.

Manifestly, precise utilization of the extremely teeny **$Cu_{0.3}Cd_{0.7}CrFeO_4$** nanocrystals protrude a new exquisite route for the promotion of echo-friendly technologies for quite delicate waste H_2O reclaiming archetypes, for surging H_2O quality and for the furtherance of effectual exertions in ameliorating treatment mechanisms.

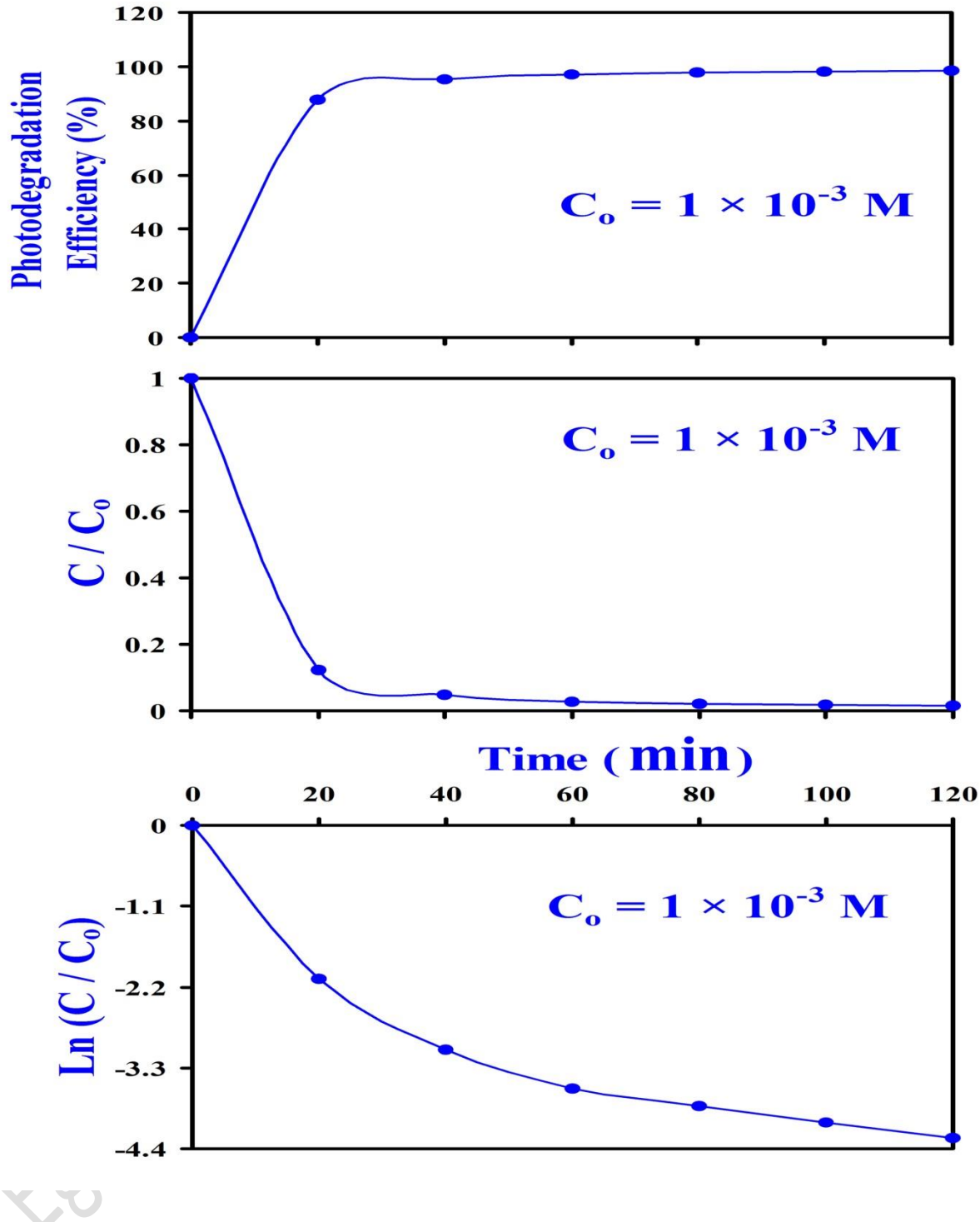

Fig. 5 Photo-catalytic efficiency and Photo-Degradation of **MB** (**1 ×10^{-3} M**) utilizing **$Cu_{0.3}Cd_{0.7}CrFeO_4$** Nano-spinels as photo-catalysts, with time duration 20 min.

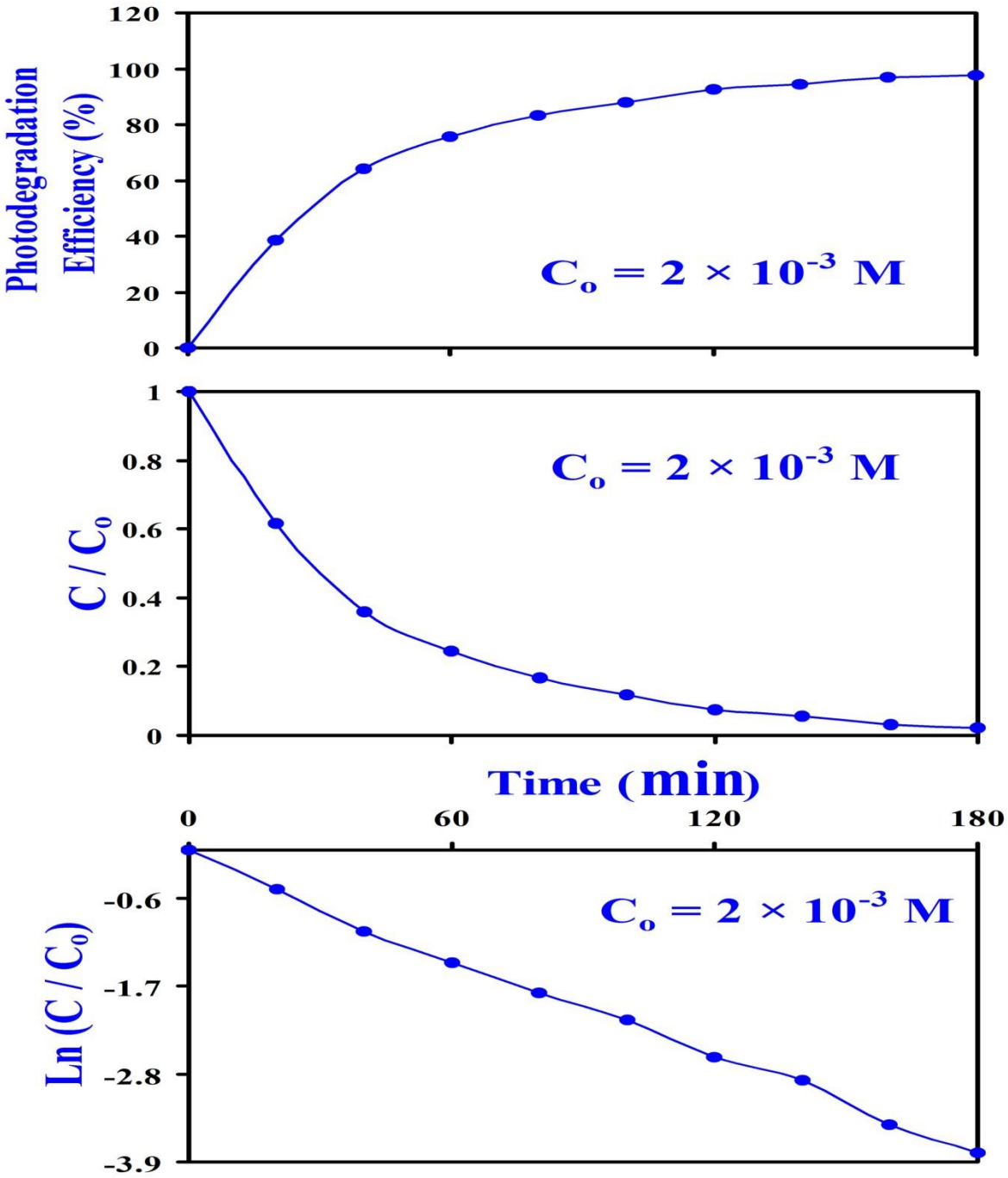

Fig. 6 Photo-catalytic efficiency and Photo-Degradation of **MB** (**2×10^{-3} M**) utilizing **$Cu_{0.3}Cd_{0.7}CrFeO_4$** Nano-spinels as photo-catalysts, with time duration 20 min.

Fig. 7 sheds light on the sequent photocatalytic degradation mechanism of Methylene Blue (**MB**) dye (**1×10^{-3} M and 2×10^{-3} M**) in aqueous solution under VL irradiation using 100 Watt Tungsten lamp fixed at ~ 10 cm distance, inspected under surging of sequent spans

of time up to 180 minutes, (time duration is 20 min), utilizing **$Cu_{0.3}Cd_{0.7}CrFeO_4$** Nano-spinel that acts as photo-catalyst.

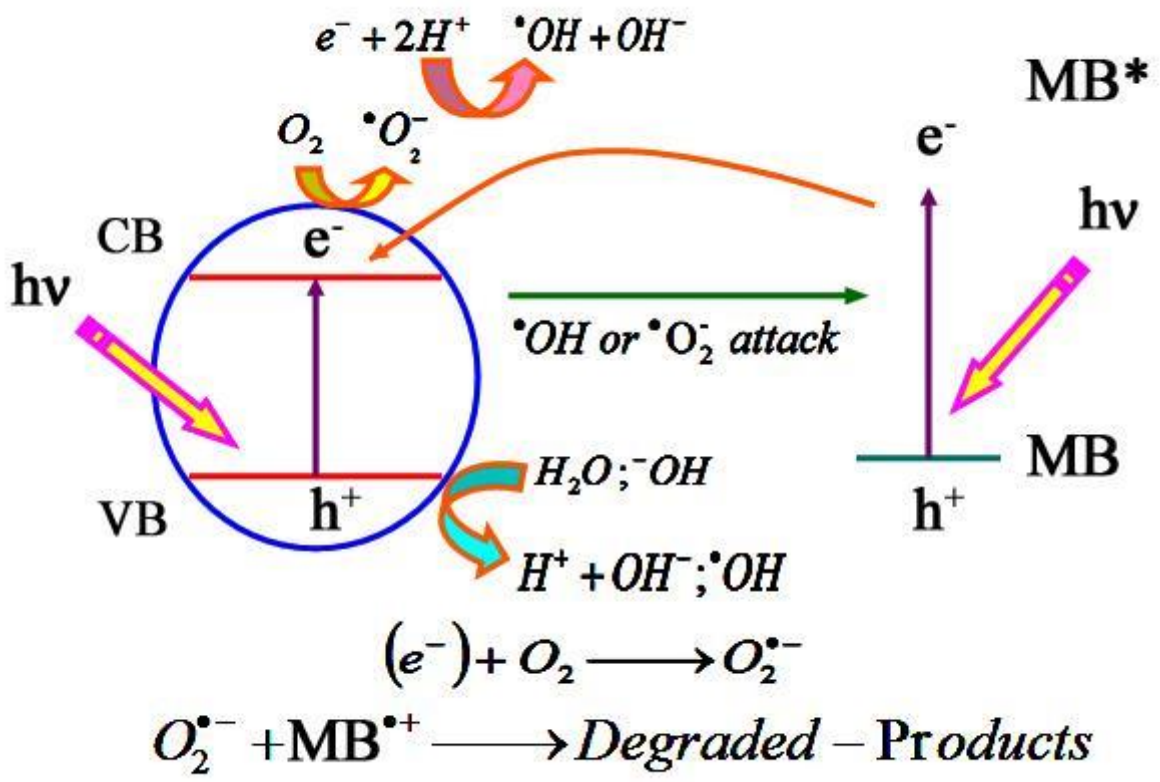

Fig. 7 The sequent photocatalytic degradation mechanism of Methylene Blue (**MB**) dye (**1×10^{-3} M and 2×10^{-3} M**), utilizing **$Cu_{0.3}Cd_{0.7}CrFeO_4$** Nano-spinel as photo-catalyst, under visible light irradiation, with time duration 20 min.

In Nano-ferrites the electrons from valency band are librated to conduction band leaving holes behind them in valency band with the aid of photons from 100 W Tungsten lamb. Electrons in conduction band unit with O2 and OH giving free radicals according to the following equations:

$$e^- + O_2 \xrightarrow{h\nu} {}^\bullet O_2^-$$

$$e^- + H_2O \xrightarrow{h\nu} H^+ + {}^\bullet OH$$

These free radicals attack MB dye with the help of photons from 100 W Tungsten lamb making degradation to the dye giving degraded products in the form of CO2 and H2O according to the following equation:

$$O_2^{\bullet -} + MB^{\bullet +} \xrightarrow{h\nu} Degraded - \text{Pr}oducts\left(H_2O + CO_2\right)$$

4. Conclusion

XRD inspection of the Ultra-teeny **$Cu_{0.3}Cd_{0.7}CrFeO_4$** emphasized the egress of single-phase spinel configuration for these nanocrystals. Crystallite size R was ~ 10.55 nm. Elicited parameters were dependent on Cu^{2+}, Cd^{2+}, Cr^{3+} and Fe^{3+} cations in these Nano-spinels. HRTEM pics provided no accumulations for nanoparticles, where average particle size value was 11.11 nm lightly rising than the crystallite size R. Photocatalytic activity for **$Cu_{0.3}Cd_{0.7}CrFeO_4$** Nano-spinels was acquired through disintegration of Methylene Blue (**MB**) dye (**1×10^{-3} M and 2×10^{-3} M**) in aqueous solution under VL irradiation using 100 Watt Tungsten lamp fixed at ~ 10 cm distance. Explicitly, utilization of **$Cu_{0.3}Cd_{0.7}CrFeO_4$** nanocrystals confirmed obvious photo-disintegration for **MB**, with excellent efficiency.

Acknowledgments

Authors are grateful for Tanta University, Faculty of Science, Egypt for scientifically supporting the current research.

5. References

[1] S.A. Kanade, Vijaya Puri, Composition dependent resistivity of thick film Ni(1−x)CoxMn2O4: (0≤x≤1) NTC thermistors, Materials Letters 60 (2006) 1428–1431, doi:10.1016/j.matlet.2005.11.042.

[2] E. Caldero´ n-Ortiz, O.Perales-Perez, P.Voyles, G.Gutierrez, M.S.Tomar, MnxZn1-xFe2-yRyO4 (R = Gd, Eu) ferrite nanocrystals for magnetocaloric applications, Microelectronics Journal 40 (2009) 677–680, doi:10.1016/j.mejo.2008.10.003.

[3] Naveen KumarSaxena, NitendarKumar, P.K.S.Pourush, Study of LiTiMg-ferrite radome for the application of satellite communication, Journal of Magnetism and Magnetic Materials 322 (2010) 2641–2646, doi:10.1016/j.jmmm.2010.03.032.

[4] S Bhukal, S Bansal, S Singhal, Magnetic Mn substituted cobalt zinc ferrite systems: Structural, electrical and magnetic properties and their role in photo-catalytic degradation of methyl orange azo dye, Physica B, 445 (2014) 48–55. http://dx.doi.org/10.1016/j.physb.2014.03.088

[5] T Li, Y Wang, Y He, J Cai, M Luo, L Zhao, Preparation and photocataytic property of $Sr_{0.25}Bi_{0.75}O_{1.36}$ photocatalyst, Mater. Letters 74 (2012) 170–172. doi:10.1016/j.matlet.2012.01.078

[6] J Zeng, J Li, J Zhong, H Yang, Y Lu, G Wang, Improved Sun light photocatalytic activity of α-Fe_2O_3 prepared with the assistance of CTAB, Materials Letters, 160 (2015) 526–528. http://dx.doi.org/10.1016/j.matlet.2015.08.037

[7] CP Yang, PA Smith, J Krupka, TW Button, The losses of microwave ferrites at communication frequencies, J**.** European Ceramic Society**,** 27 (2007) 2765-2770. doi:10.1016/j.jeurceramsoc.2006.11.004

[8] E Casbeer, VK Sharma, X-Z Li, Synthesis and Photocatalytic Activity of Ferrites under Visible Light: A Review, Separation and Purification Technology, 87 (2012) 1-14. doi:10.1016/j.seppur.2011.11.034

[9] A I Ghoneim, T M Meaz, Structural and ferri-magnetic features of the nano-crystalline Mn0.5CdxSr0.5-xFe2O4 nanoparticles, IOP Conf. Series: Journal of Physics: Conf. Series 1253 (2019) 012019, doi:10.1088/1742-6596/1253/1/012019.

[10] MA Amer, TM Meaz, SS Attalah, AI Ghoneim, Structural and magnetic characterization of the $Mg_{0.2-x}Sr_xMn_{0.8}Fe_2O_4$ nanoparticles, J. Magn. Magn. Mater., 363 (2014) 60–65. http://dx.doi.org/10.1016/j.jmmm.2014.03.067

[11] SS Thakur, A Pathania, P Thakur, A Thakur, J-H Hsu, Improved structural, electrical and magnetic properties of Mn-Zn-Cd nanoferrites, Ceram. Intern., 41 (2015) 5072-5078. http://dx.doi.org/10.1016/j.ceramint.2014.12.077

[12] KK Bamzai, G Kour, B Kaur, M Arora, RP Pant, Infrared spectroscopic and electron paramagnetic resonance studies on Dy substituted magnesium ferrite, J. Magn. Magn. Mater., 345 (2013) 255–260. http://dx.doi.org/10.1016/j.jmmm.2013.07.002

[13] KB Modi, SJ Shah, NB Pujara, TK Pathak, NH Vasoya, IG Jhala, Infrared spectral evolution, elastic, optical and thermodynamic properties study on mechanically milled $Ni_{0.5}Zn_{0.5}Fe_2O_4$ spinel ferrite, J. Mol. Str., 1049 (2013) 250–262. http://dx.doi.org/10.1016/j.molstruc.2013.06.051

[14] Q Wu, H Yang, H Zhu, Z Gao, Construction of CNCs-TiO_2 heterojunctions with enhanced photocatalytic activity for crystal violet removal, Optik, 179 (2019) 195-206. https://doi.org/10.1016/j.ijleo.2018.10.153

[15] M Rahimi, M Eshraghi, P Kameli, Structural and magnetic characterizations of Cd substituted nickel ferrite nanoparticles, Ceram. Intern., 40 (2014) 15569–15575. http://dx.doi.org/10.1016/j.ceramint.2014.07.033

[16] A I Ghoneim, T M Meaz, H A Aboelkhir, Structural, thermal and ferrimagnetic studies of the as-fabricated La^{3+}-doped Co-nano-spinels, IOP Conf. Series: Journal of Physics: Conf. Series 1253 (2019) 012020, doi:10.1088/1742-6596/1253/1/012020.

[17] G Dixit, JP Singh, RC Srivastava, HM Agrawal, Magnetic resonance study of Ce and Gd doped $NiFe_2O_4$ nanoparticles, J. Magn. Magn. Mater., 324 (2012) 479–483. doi:10.1016/j.jmmm.2011.08.027

[18] MA Amer, TM Meaz, SS Attalah, AI Ghoneim, Structural phase transition of as-synthesized Sr–Mn nanoferrites by annealing temperature, J. Magn. Magn. Mater., 393 (2015) 467–478. http://dx.doi.org/10.1016/j.jmmm.2015.06.013

[19] BD Cullity, Elements of X-ray diffraction, Second Edition, Addison-Wesley Publishing Company, INC, United States of America, Congress catalog No 56-10137, (1978).

[20] M.A. Amer, T.M. Meaz, S.S. Attalah, A.I. Ghoneim, Annealing effect on structural phase transition of as-synthesized Mg0.1Sr0.1Mn0.8Fe2O4 nanoparticles, Journal of Alloys and Compounds 654 (2016) 45-55, http://dx.doi.org/10.1016/j.jallcom.2015.09.114.

[21] V Kumar, Y Ali, RG Sonkawade, AS Dhaliwal, Effect of gamma irradiation on the properties of plastic bottle sheet, Nucl. Instrum. Methods Phys. Res. Sec. B, 287 (2012) 10-14. http://dx.doi.org/10.1016/j.nimb.2012.07.007

[22] N Lenin, RR Kanna, K Sakthipandi, AS Kumar, Structural, electrical and magnetic properties of $NiLa_xFe_{2-x}O_4$ Nanoferrites, Mater. Chem. and Phys. 212 (2018) 385–393. 212:385-393. DOI: 10.1016/j.matchemphys.2018.03.062

[23] BD Cullity, Introduction to magnetic materials. Addison-Wesley Publishing, Inc., Boston, (1972).

[24] M Hashim, KS Alimuddin, SE Shirsath, RK Kotnala, H Chung, R Kumar, Structural properties and magnetic interactions in $Ni_{0.5}Mg_{0.5}Fe_{2-x}Cr_xO_4$ ($0 \leq x \leq 1$) ferrite nanoparticles, Powder Technology, 229 (2012) 37–44. doi:10.1016/j.powtec.2012.05.054

[25] SA Saafan, TM Meaz, EH El-Ghazzawy, MK El Nimr, MM Ayad, M Bakr, A.C. and D.C. conductivity of NiZn ferrite nanoparticles in wet and dry conditions. J. Magn. Magn. Mater., 322 (2010) 2369–2374. doi:10.1016/j.jmmm.2010.02.039

[26] SM Patange, SE Shirsath, KS Lohar, SG Algude, SR Kamble, N Kulkarni, DR Mane, KM Jadhav, Infrared spectral and elastic moduli study of $NiFe_{2-x}Cr_xO_4$ nanocrystalline ferrites. J. Magn. Magn. Mater., 325 (2013) 107–111. http://dx.doi.org/10.1016/j.jmmm.2012.08.022

[27] SM Patange, SE Shirsath, SP Jadhav, VS Hogade, SR Kamble, KM Jadhav, Elastic properties of nanocrystalline aluminium substituted nickel ferrites prepared by co-precipitation method. J. Mol. Str., 1038 (2013) 40–44. http://dx.doi.org/10.1016/j.molstruc.2012.12.053

[28] I Sharifi, H Shokrollahi, Structural, Magnetic and Mössbauer evaluation of Mn substituted Co–Zn ferrite nanoparticles synthesized by co-precipitation, J. Magn. Magn. Mater., 334 (2013) 36–40. http://dx.doi.org/10.1016/j.jmmm.2013.01.021

[29] K Shetty, SV Lokesh, D Rangappa, HP Nagaswarupa, H Nagabhushana, KS Anantharaju, SC Prashantha, YS Vidya, SC Sharma, Designing $MgFe_2O_4$ decorated on green mediated reduced graphene oxide sheets showing photocatalytic performance and luminescence property, Physica B, 507 (2017) 67–75. http://dx.doi.org/10.1016/j.physb.2016.11.021

[30] S Rajoriya, S Bargole, S George, VK Saharan, PR Gogate, AB Pandit, Synthesis and characterization of Samarium and Nitrogen doped TiO_2 photocatalysts for photo-degradation of 4-Acetamidophenol in combination with hydrodynamic and acoustic cavitation, Sep. Pur. Tech., 209 (2019) 254–269. https://doi.org/10.1016/j.seppur.2018.07.036